

Hard Exclusive Meson Production at COMPASS



Kamil Augsten

on behalf of the COMPASS Collaboration

Czech Technical University in Prague

kamil.augsten@cern.ch



Introduction

- ❖ Hard Exclusive Meson Production (HEMP)

- ❖ tool to study mechanism of reaction or structure of nucleon

- ❖ described by Generalized Parton Distributions (GPDs) - provide important information

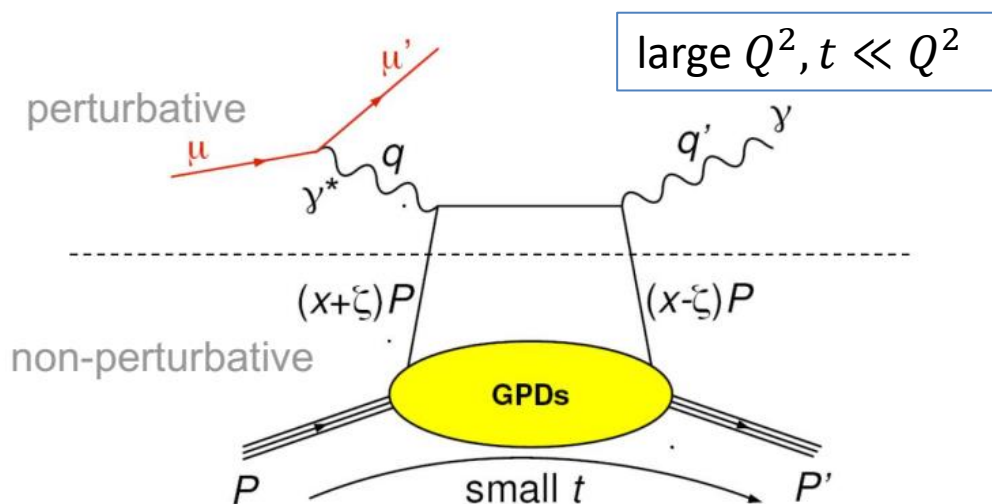
- ❖ GPDs give access to 3D partonic structure of a hadron

- ❖ HEMP complementary to DVCS

$$\ell N \rightarrow \ell' N' M$$

$$\gamma^* N \rightarrow N' M \text{ (one-photon approx.)}$$

‘hard’ = high virtuality Q^2 of γ^* or large meson mass



		Quark Polarization		
		U	L	T
Nucleon Polarization	U	H		\bar{E}_T
	L		\tilde{H}	\tilde{E}_T
	T	E	\tilde{E}	$H_T \tilde{H}_T$

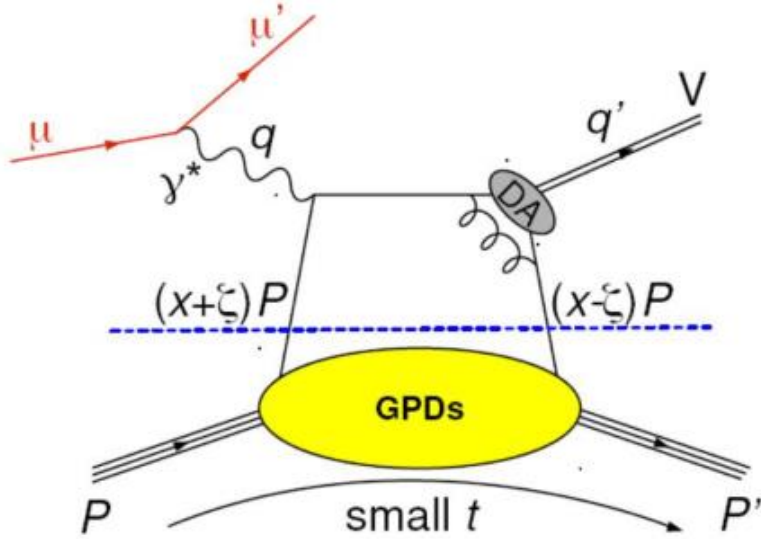
$H, E, \tilde{H}, \tilde{E}$: chiral-even GPDs (parton helicity conserved)

$\bar{E}_T, \tilde{E}_T, H_T, \tilde{H}_T$: chiral-odd (transversity) GPDs (parton helicity flipped)

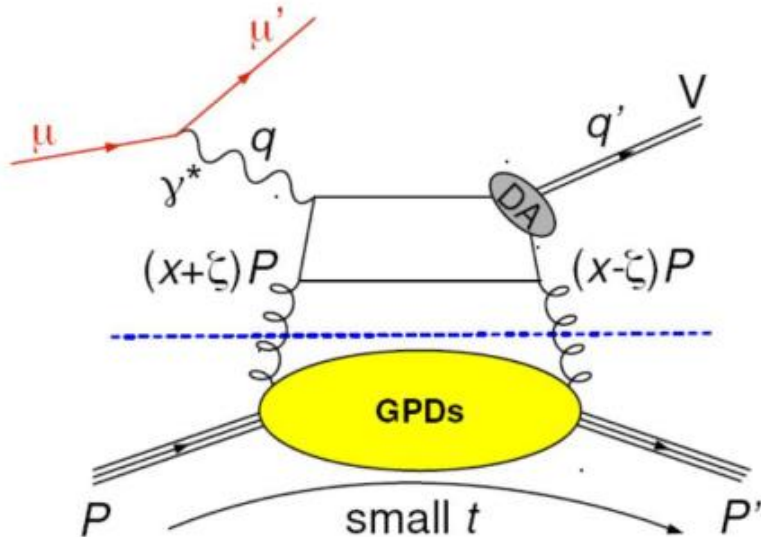
$$\bar{E}_T = 2\tilde{H}_T + E_T$$

GPDs and Hard Exclusive Meson Production

quark contribution



gluon contribution



- ❖ wave function of meson (DA) non-perturbative
- ❖ quark and gluon contribution at the same order in α_s for vector mesons
- ❖ flavour separation – constraints for partonic specific GPDs due dif. meson partonic structure
 - ❖ vector mesons mainly sensitive to $H^{q,g}, E^{q,g}(x, \xi, t)$
 - ❖ pseudoscalar mesons sensitive to $\tilde{H}^{q,g}, \tilde{E}^{q,g}(x, \xi, t)$
 - ❖ + all mesons to $\bar{E}_T^q(x, \xi, t)$ and $H_T^q(x, \xi, t)$

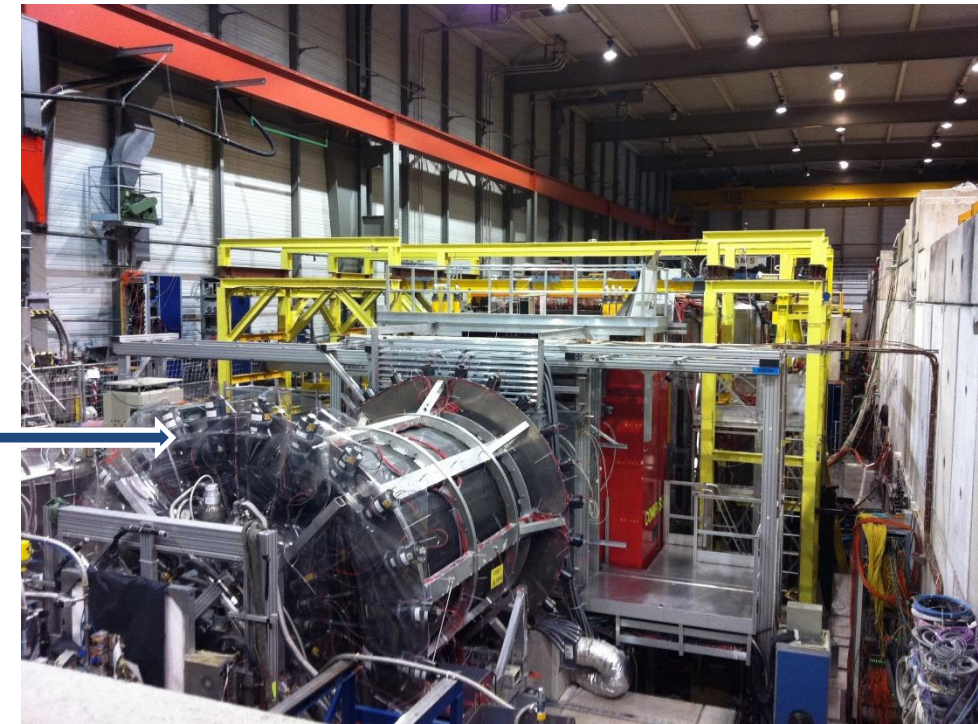
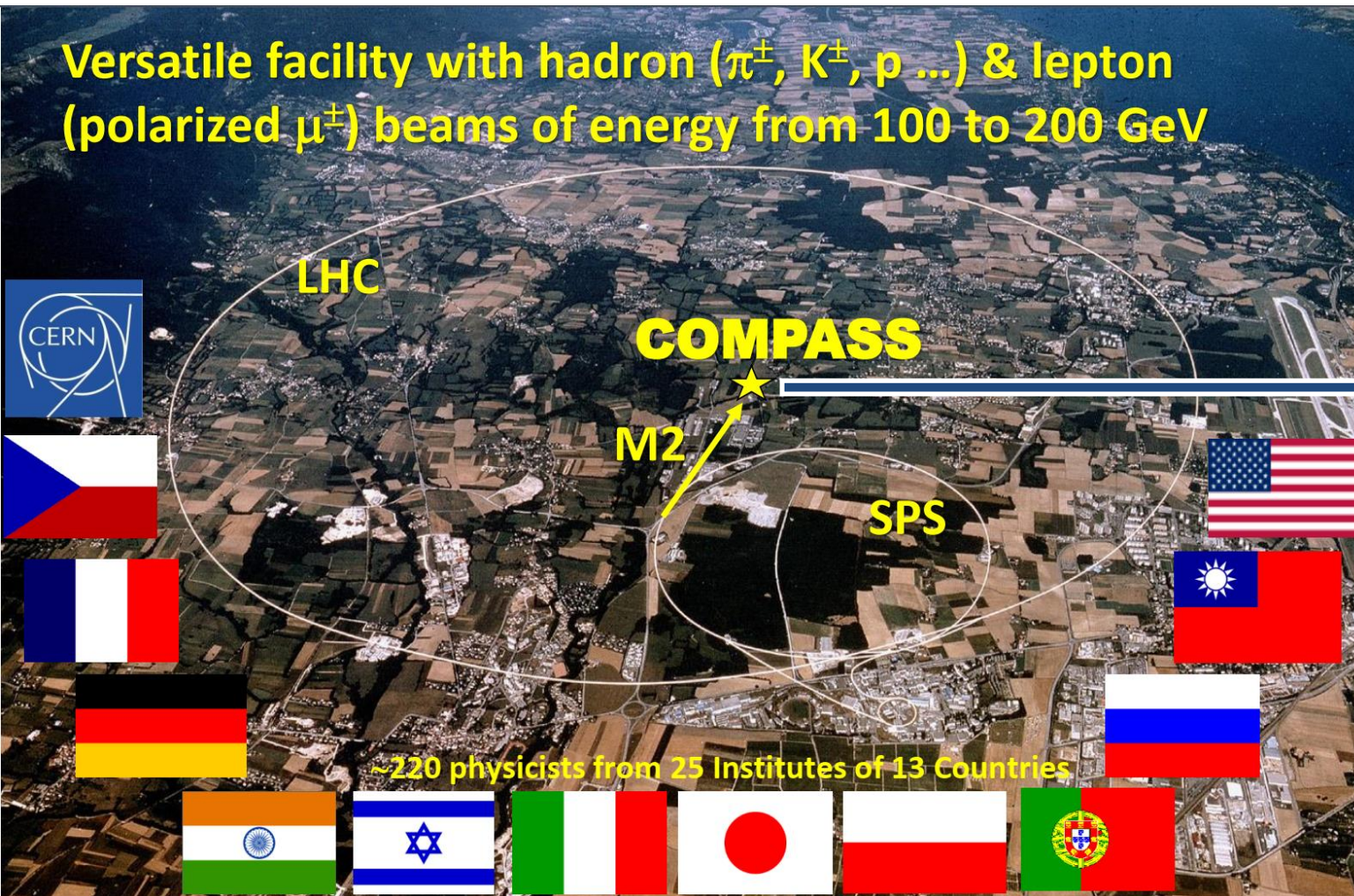
$$\text{❖ } E_{\rho_0} = \frac{1}{\sqrt{2}} \left(\frac{2}{3} E^u + \frac{1}{3} E^d + \frac{3}{4} E^g / x \right)$$

$$\text{❖ } E_{\omega} = \frac{1}{\sqrt{2}} \left(\frac{2}{3} E^u - \frac{1}{3} E^d + \frac{1}{4} E^g / x \right)$$

COMPASS Experiment

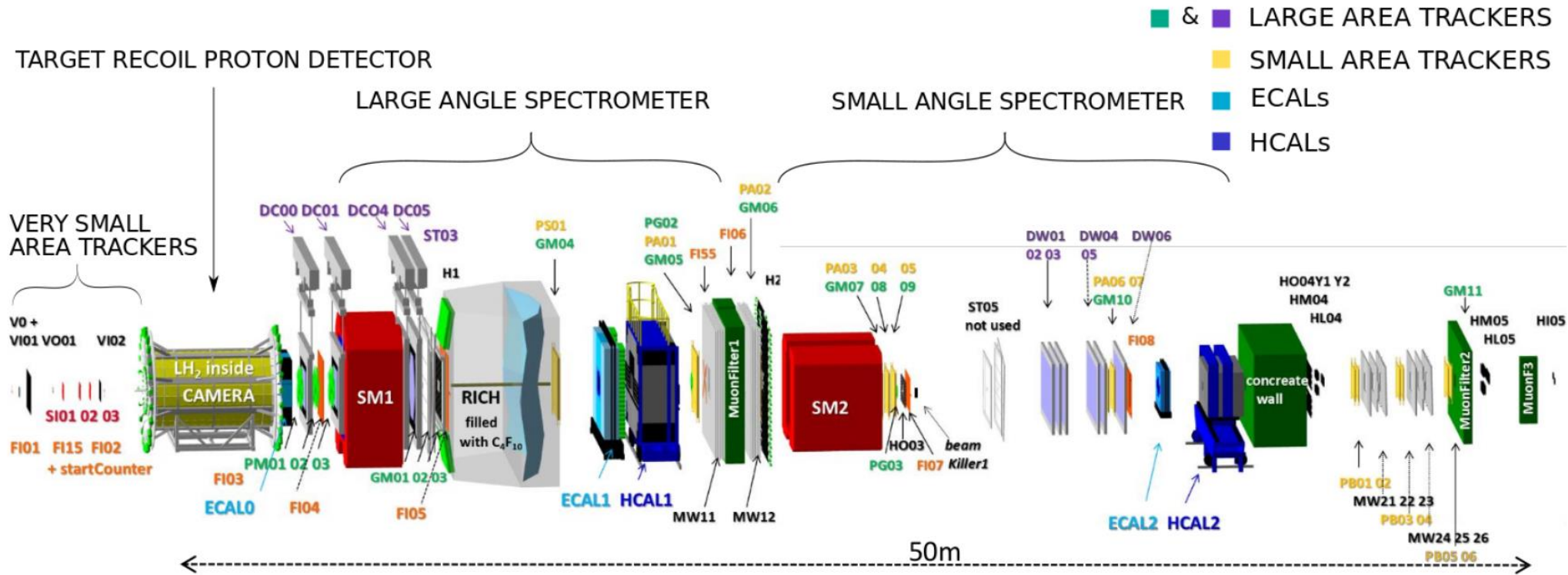
COmmon **M**uon **P**roton **A**pparatus for **S**tructure and **S**pectroscopy

Versatile facility with hadron (π^\pm , K^\pm , p ...) & lepton (polarized μ^\pm) beams of energy from 100 to 200 GeV



data taking 2002 – 2022 & longitudinally, transversely or unpolarized targets

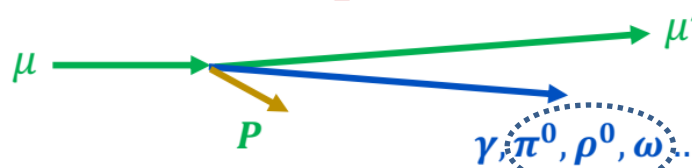
COMPASS Experiment – setup and data



NIMA 577 (2007)
455–518
&
NIMA 779 (2015)
69

μ^+ , μ^- beams
- data separately
polarization $\sim \pm 80\%$
energy 160 GeV

Exclusive Muoproduction



2.5m long LH_2 target

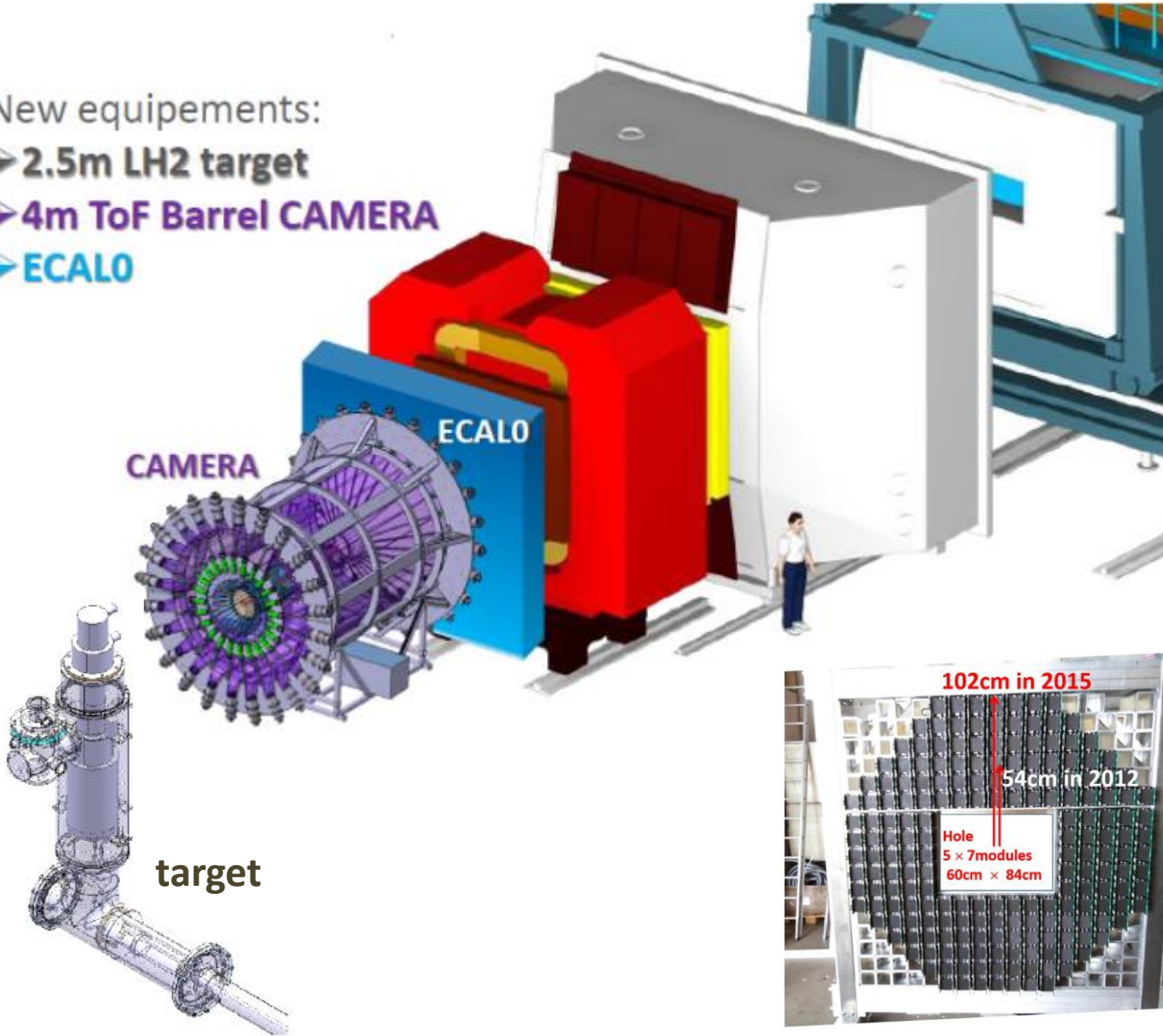
results in this talk: data from 2012 pilot run (4 weeks) and 2016 run

Hard Exclusive Meson Production (HEMP)

Key parts of setup

New equipments:

- 2.5m LH2 target
- 4m ToF Barrel CAMERA
- ECALO

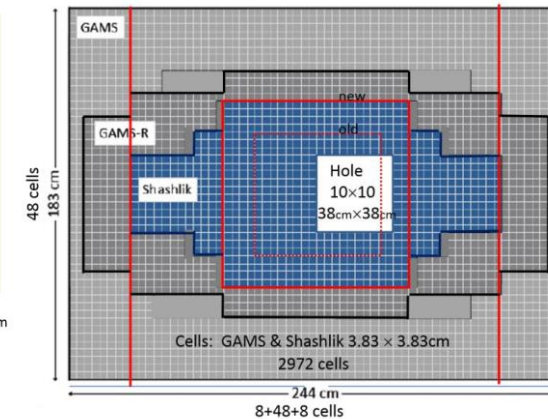
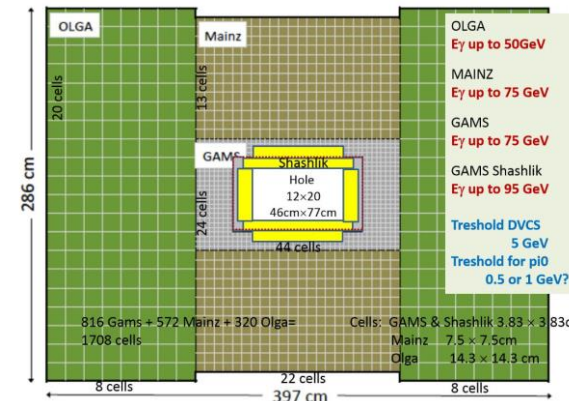
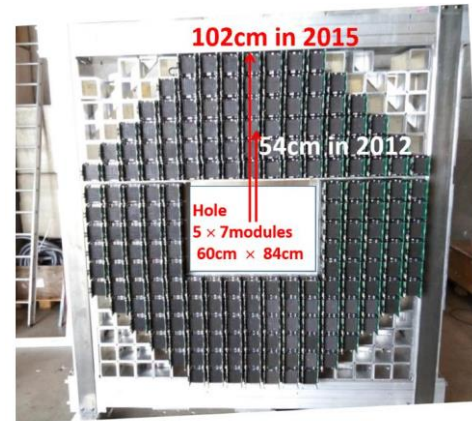
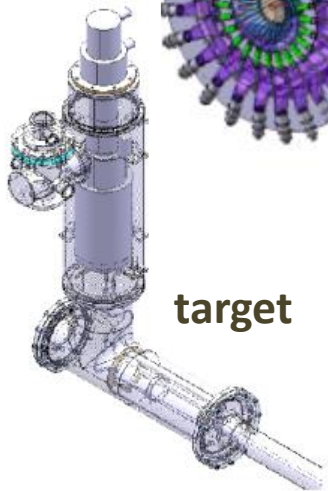


❖ Target ToF system (CAMERA)

- ❖ 24 inner and 24 outer scintillators
- ❖ 1 GHz readout and 310ps ToF resolution

❖ Particle ID:

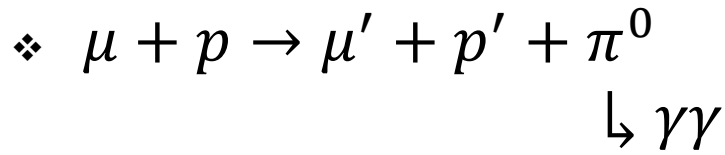
- ❖ Ring Imaging Cherenkov (RICH) detector
- ❖ EM calorimeters (ECALO 0-40 mrad, ECAL1 40-150 mrad, ECAL2 150-300 mrad)
- ❖ Hadronic calorimeters (HCAL1, HCAL2)
- ❖ 2 muon walls



Selection π_0

2016 run

- ❖ topology: scattered muon + two neutral clusters in calorimeters + recoil proton candidate



- ❖ $1 < Q^2 < 5 \text{ (GeV/c)}^2$

- ❖ $8.5 < \nu < 28 \text{ GeV}$

- ❖ $0.08 < |t| < 0.64 \text{ (GeV/c)}^2$

- ❖ transverse momentum constraint:

$$\Delta p_T = p_{T,spect}^p - p_{T,recoil}^p$$

- ❖ $\Delta\phi = \phi_{spect}^p - \phi_{recoil}^p$

- ❖ z-coordinate of inner CAMERA ring:

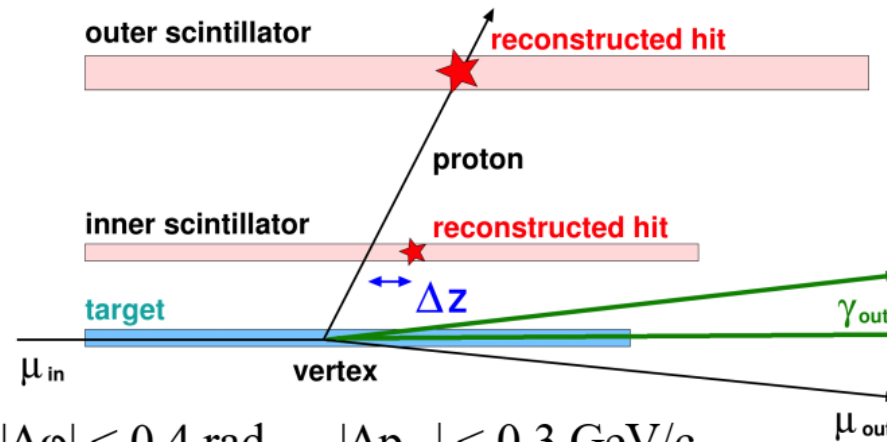
$$\Delta z = z_{spect}^p - z_{recoil}^p$$

- ❖ energy-momentum conservation:

$$M_X^2 = (p_\mu + p_p - p_{\mu'} - p_{p'} - p_{\pi^0})^2$$

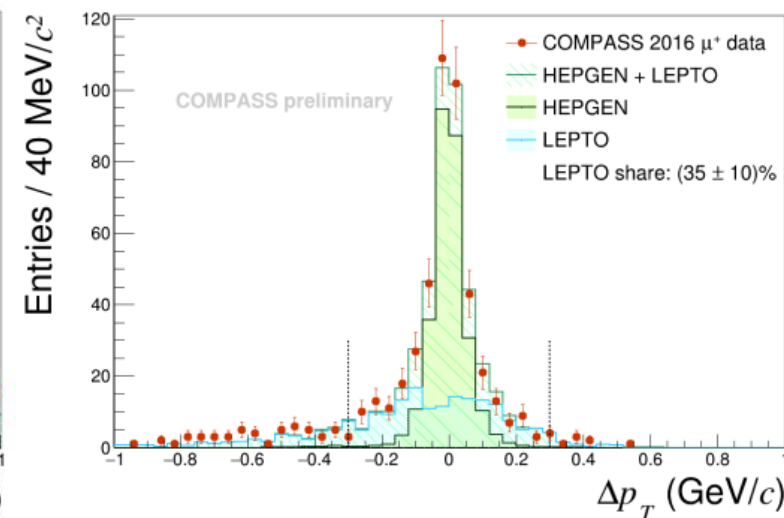
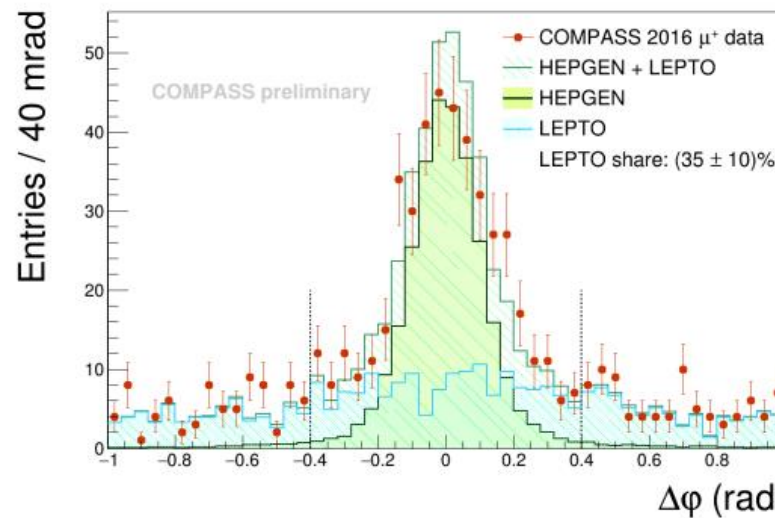
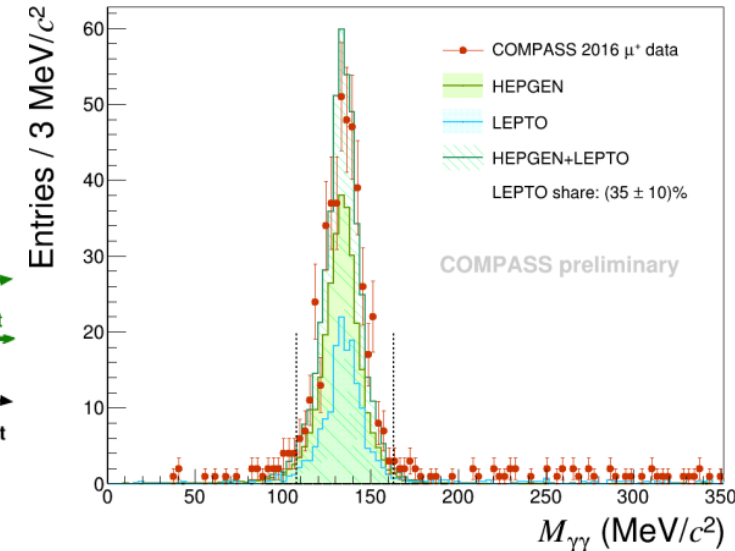
- ❖ invariant mass $M_{\gamma\gamma}$ (108, 163) MeV/c^2

- ❖ kinematic fit



$$|\Delta\phi| < 0.4 \text{ rad} \quad |\Delta p_T| < 0.3 \text{ GeV/c}$$

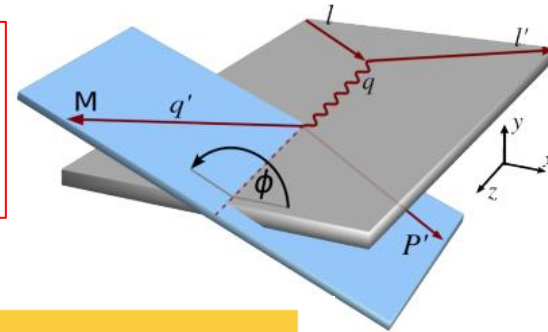
$$|\Delta Z_A| < 16 \text{ cm} \quad |M_X^2| < 0.3 \text{ (GeV/c}^2)^2$$



exclusive π_0 HEMP cross-section

❖ μp cross-section reduced to $\gamma^* p$ $\frac{d^4\sigma_{\mu p}}{dQ^2 dt d\nu d\phi} = \Gamma \frac{d^2\sigma_{\gamma^* p}}{dt d\phi}$ $\Gamma = \Gamma(E_\mu, Q^2, \nu)$

$$\frac{d\sigma_{\gamma^* p}}{dt d\phi} = \frac{1}{2\pi} \left[\frac{d\sigma_T}{dt} + \epsilon \frac{d\sigma_L}{dt} + \epsilon \cos(2\phi) \frac{d\sigma_{TT}}{dt} + \sqrt{2\epsilon(1+\epsilon)} \cos(\phi) \frac{d\sigma_{LT}}{dt} \right]$$



❖ spin independent cross-section after averaging:

$$\frac{d^2\sigma_{\gamma^* p}}{dt d\phi} = \frac{1}{2} \left(\frac{d^2\sigma_{\gamma^* p}^{\leftarrow}}{dt d\phi} + \frac{d^2\sigma_{\gamma^* p}^{\rightarrow}}{dt d\phi} \right) \Rightarrow \text{study } \phi \text{ dependence}$$

❖ after integration in ϕ

$$\frac{d\sigma_T}{dt} + \epsilon \frac{d\sigma_L}{dt} \Rightarrow \text{study } t \text{ dependence}$$

❖ measurement in 2012 pilot run published:
PLB 805 (2020) 135454

GPDs in exclusive π^0 production

$$\frac{d\sigma_L}{dt} \propto \left[(1 - \xi^2) |\langle \tilde{\mathcal{H}} \rangle|^2 - 2\xi^2 \text{Re}(\langle \tilde{\mathcal{H}} \rangle^* \langle \tilde{\mathcal{E}} \rangle) - \frac{t'}{4M^2} \xi^2 |\langle \tilde{\mathcal{E}} \rangle|^2 \right]$$

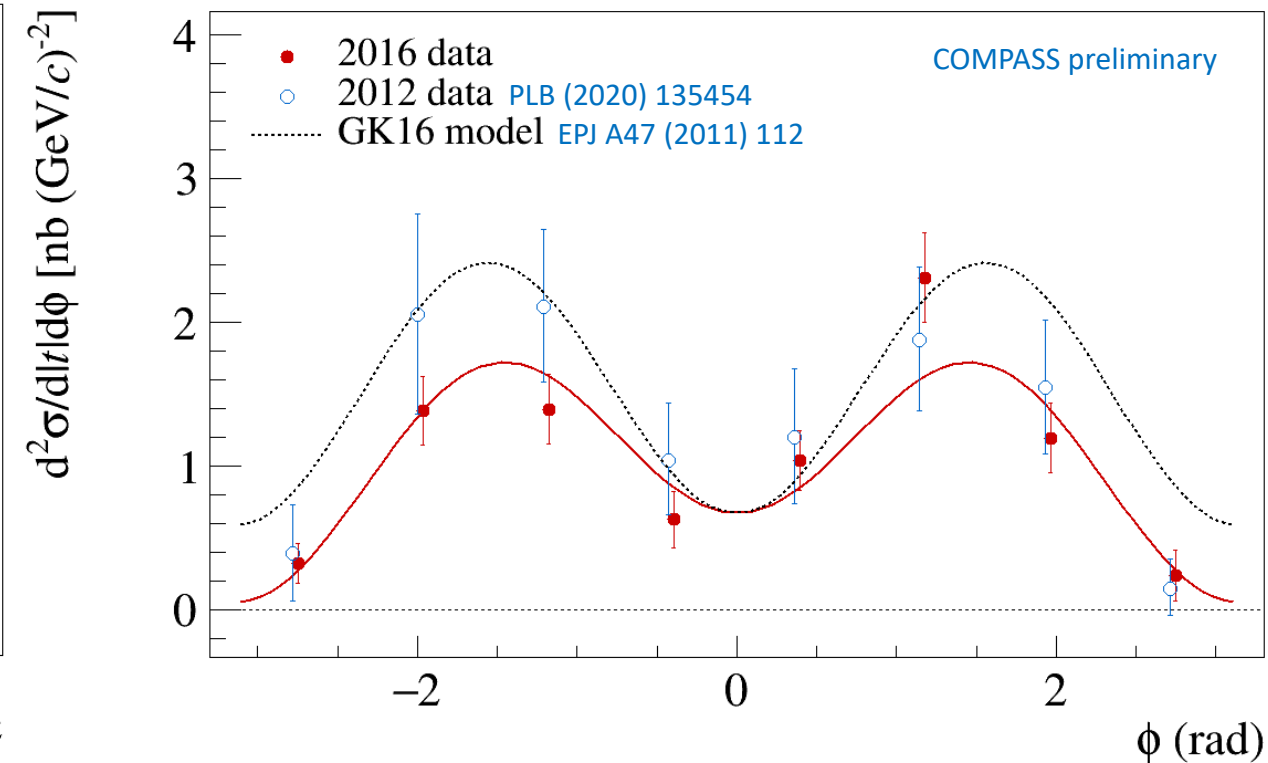
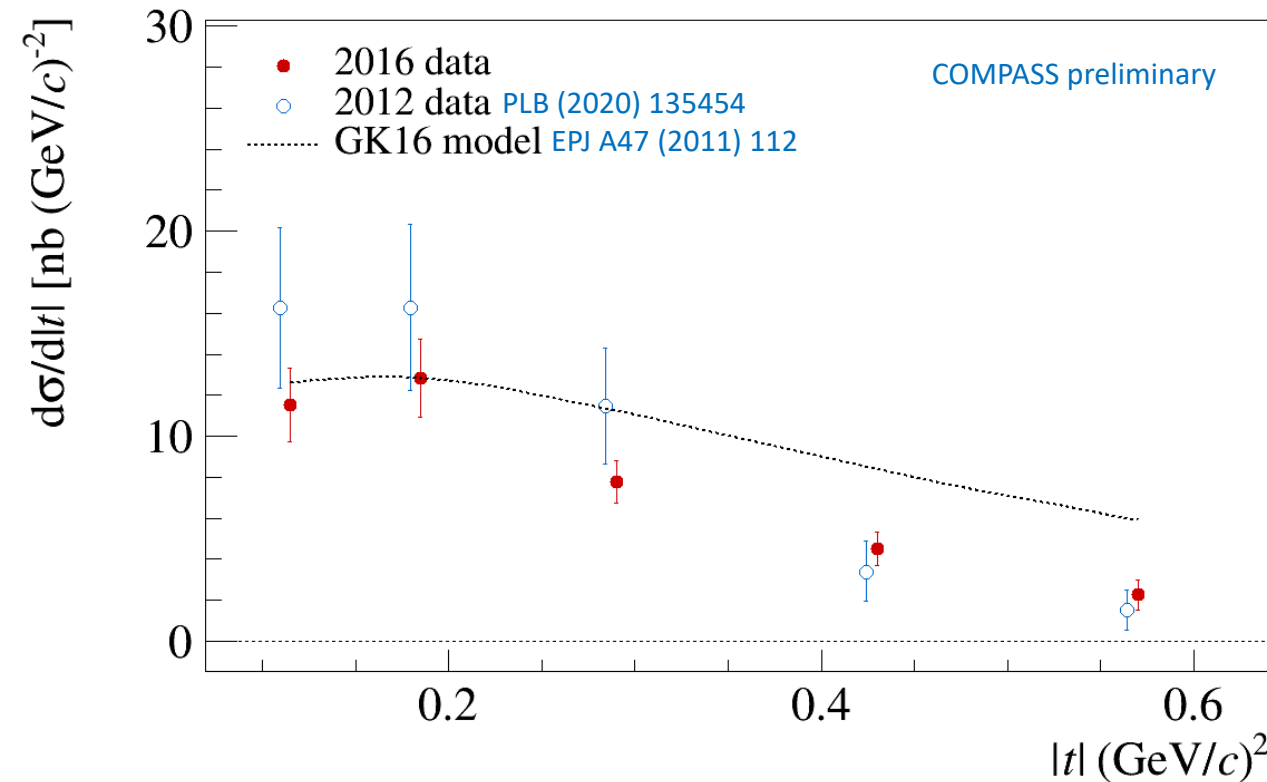
$$\frac{d\sigma_T}{dt} \propto \left[(1 - \xi^2) \langle \mathcal{H}_T \rangle^2 - \frac{t'}{8M^2} \langle \bar{\mathcal{E}}_T \rangle^2 \right]$$

$$\frac{d\sigma_{TT}}{dt} \propto t' \langle \bar{\mathcal{E}}_T \rangle^2$$

$$\frac{d\sigma_{LT}}{dt} \propto \xi \sqrt{1 - \xi^2} \sqrt{-t'} \text{Re}(\langle \mathcal{H}_T \rangle^* \langle \tilde{\mathcal{E}} \rangle)$$

exclusive π_0 HEMP cross-section - results

- ❖ t -dependence and ϕ -dependence of exclusive π_0 cross-section on unpolarized proton target – at low ξ ($\langle x_B \rangle = 0.096$), input for phenomenological models, large impact on constraining chiral-odd GPD (especially the poorly known \bar{E}_T)
- ❖ shown 2016 results are 2.3x larger statistic than 2012, full 2016/17 can be 9x larger



Selection ρ_0 and ω

2012 pilot run

Common selection: $1 < Q^2 < 10$ (GeV/c)², $W > 5$ GeV/c², $0.01 < p_T^2 < 0.5$ (GeV/c)², $0.1 < y < 0.9$
 Recoil proton detector not included in selection

$\mu + p \rightarrow \mu' + p' + \omega$ EPJC 81 (2021) 126
 $\hookrightarrow \pi^+ + \pi^- + \pi^0$ Branching ratio $\approx 89\%$
 $\hookrightarrow \gamma_l + \gamma_h$ Branching ratio $\approx 99\%$

$0.1 < M_{\gamma\gamma} < 0.17$ GeV, $0.71 < M_{\pi^+\pi^-\pi^0} < 0.86$ GeV

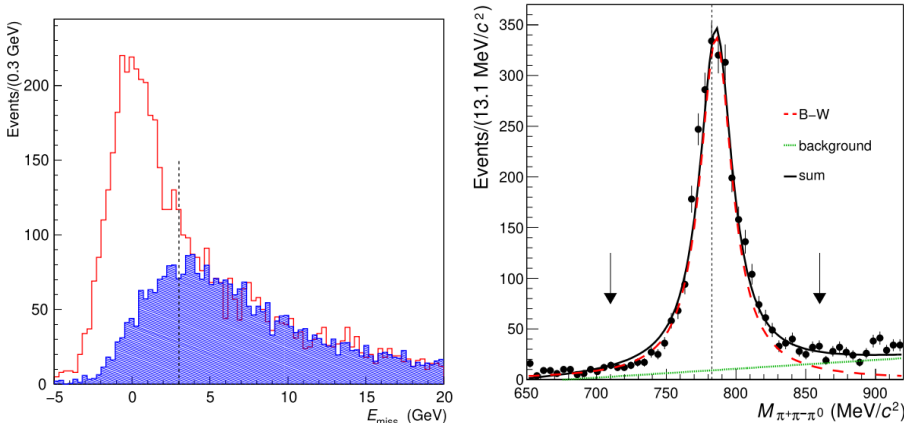
topology:

scattered muon + two hadrons with opposite charges
 + two neutral clusters in calorimeters

event yield: 3060 events

$$|E_{\text{miss}}| < 3 \text{ GeV}$$

$$E_{\text{miss}} = \frac{M_X^2 - M^2}{2M}$$

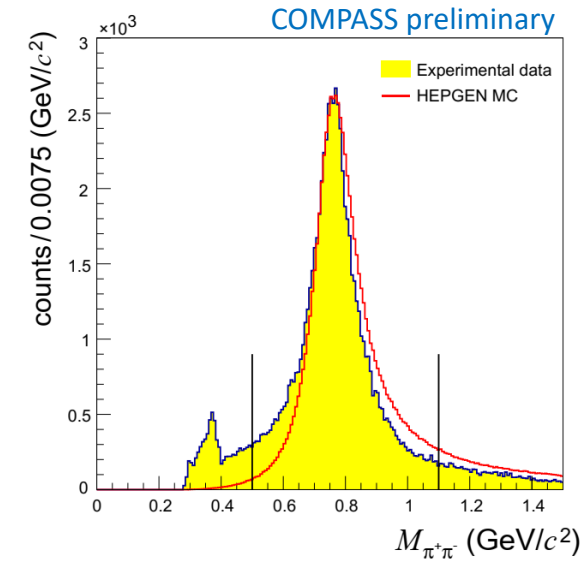
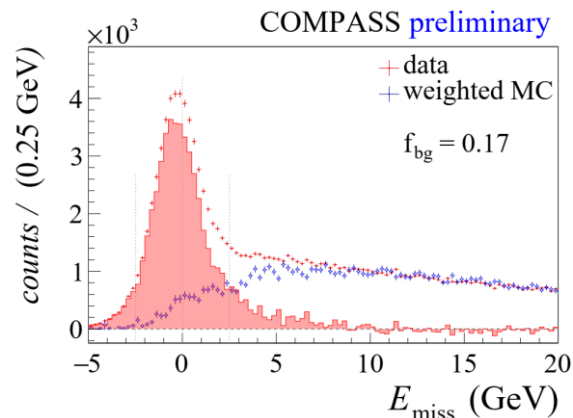


$\mu + p \rightarrow \mu' + p' + \rho^0$ Preliminary
 $\hookrightarrow \pi^+ + \pi^-$ Branching ratio $\approx 99\%$
 $0.5 < M_{\pi^+\pi^-} < 1.1$ GeV

topology:

scattered muon + two hadrons with opposite charges
 event yield: 52257 events

exclusivity: $|E_{\text{miss}}| < 2.5$ GeV



Vector meson spin-density matrix

$$\rho_{\lambda_V \lambda'_V} = \frac{1}{2N} \sum_{\lambda_\gamma \lambda'_\gamma \lambda_N \lambda'_N} F_{\lambda_V \lambda'_N \lambda_\gamma \lambda_N} \mathcal{Q}_{\lambda_\gamma \lambda'_\gamma}^{U+L} F_{\lambda'_V \lambda'_N \lambda'_\gamma \lambda_N}^*$$

helicity of vector meson V
helicities of virtual photon γ and nucleon N

photon spin density matrix ($\mu \rightarrow \mu' + \gamma^*$); calculable on QED

$$\mathcal{Q}_{\lambda_\gamma \lambda'_\gamma}^{U+L} = \mathcal{Q}_{\lambda_\gamma \lambda'_\gamma}^U + P_b \mathcal{Q}_{\lambda_\gamma \lambda'_\gamma}^L$$

- ❖ F helicity amplitudes describe transitions $\lambda_\gamma, \lambda_N \rightarrow \lambda_V, \lambda'_N$, depend on W, Q^2, p_T^2
- ❖ $\rho_{\lambda_V \lambda'_V}$ decomposes into 9 matrices $\rho_{\lambda_V \lambda'_V}^\alpha$ corresponding to different photon polarization states ($\alpha=0-3$ transverse, $\alpha=4$ longitudinal, $\alpha=5-8$ interference amplitudes)
- ❖ if not possible to separate long. and transv. photon contributions, SDMEs are defined:

$$r_{\lambda_V \lambda'_V}^{04} = (\rho_{\lambda_V \lambda'_V}^0 + \epsilon R \rho_{\lambda_V \lambda'_V}^4)(1 + \epsilon R)^{-1}, \quad r_{\lambda_V \lambda'_V}^\alpha = \begin{cases} \rho_{\lambda_V \lambda'_V}^\alpha (1 + \epsilon R)^{-1}, & \alpha = 1, 2, 3, \\ \sqrt{R} \rho_{\lambda_V \lambda'_V}^\alpha (1 + \epsilon R)^{-1}, & \alpha = 5, 6, 7, 8. \end{cases}$$

$R = d\sigma_L/d\sigma_T$ diff. longitudinal-to-transverse cross-section ratio of virtual photons
and ϵ is the virtual-photon polarization parameter

↓
23 SDMEs

Vector Meson SDMEs and GPDs

- ❖ access to helicity amplitudes F allows:
 - ❖ test of s-channel helicity conservation SCHC ($\lambda_\gamma = \lambda_V$)
 - ❖ decomposition into Natural (N) and Unnatural (U) Parity Exchange (NPE/UPE)
in Regge framework: NPE $J^P = (0^+, 1^-, \dots)$ (pomeron, ρ , ω , $a_2 \dots$); UPE $J^P = (0^-, 1^+, \dots)$ (π , $a_1 \dots$)
 - ❖ quantify the role of transitions with helicity flip $F_{\lambda_V \lambda'_N \lambda_\gamma \lambda_N} = T_{\lambda_V \lambda'_N \lambda_\gamma \lambda_N} + U_{\lambda_V \lambda'_N \lambda_\gamma \lambda_N}$
 - ❖ determination of the longitudinal-to-transverse cross-section ratio
 - ❖ test of GPD models
 - like SCHC-violating transitions $\gamma_T \rightarrow V_L$ to test sensitivity to GPDs with helicity-flip of „active“ quark (transversity GPDs)
- ❖ GPDs in HEMP:
 - ❖ 4 chiral-even and 4 chiral-odd/transversity (not in DVCS)
 - ❖ universality of GPDs, quark flavor filter, insights into reaction mechanism

Experimental access to SDMEs

- ❖ through angular distribution K. Schilling and G. Wolf, Nucl. Phys. B **61**, 381(1973) ρ_0

$$\mathcal{W}^{U+L}(\Phi, \phi, \cos \Theta) = \mathcal{W}^U(\Phi, \phi, \cos \Theta) + P_b \mathcal{W}^L(\Phi, \phi, \cos \Theta)$$

- ❖ decomposition into 23 terms with different angular dependences

- ❖ 15 unpolarized - \mathcal{W}^U and 8 polarized - \mathcal{W}^L

- ❖ extraction of SDMEs:

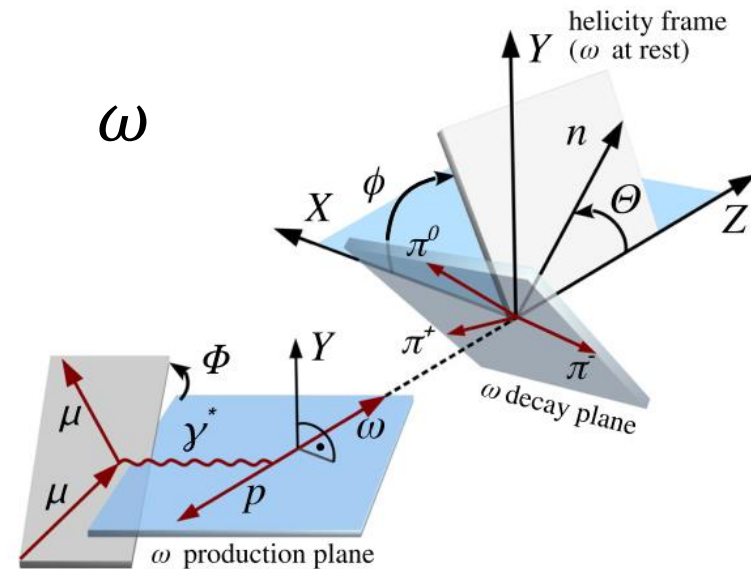
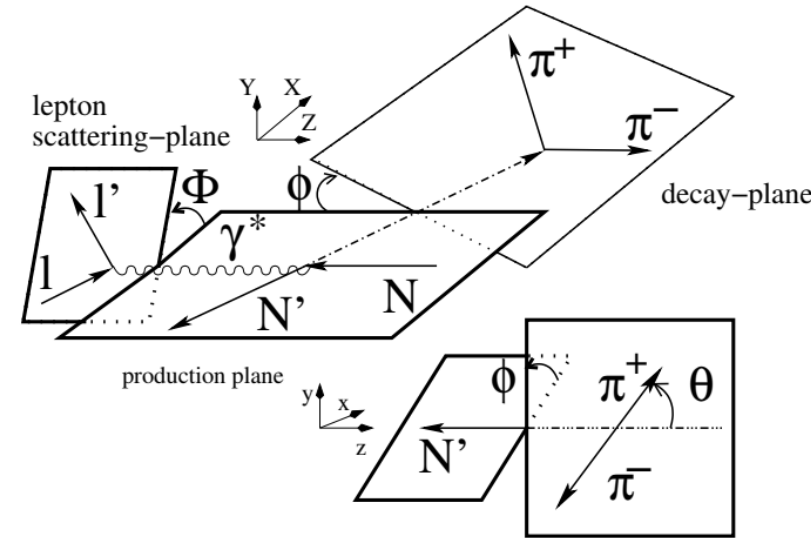
- ❖ Unbinned Maximum Likelihood fit to experimental function $\mathcal{W}(\mathcal{R}, \Phi, \phi, \cos \Theta)$, \mathcal{R} is set of 23 SDMEs

- ❖ total acceptance

- ❖ fraction of background f_{bg}

- ❖ angular distribution of background

$$\mathcal{W}^{U+L}(\mathcal{B}, \Phi, \phi, \cos \Theta)$$



Results

$1 < Q^2 < 10 \text{ (GeV/c)}^2$
 $5 < W < 17 \text{ GeV/c}^2$
 $0.01 < p_T^2 < 0.5 \text{ (GeV/c)}^2$

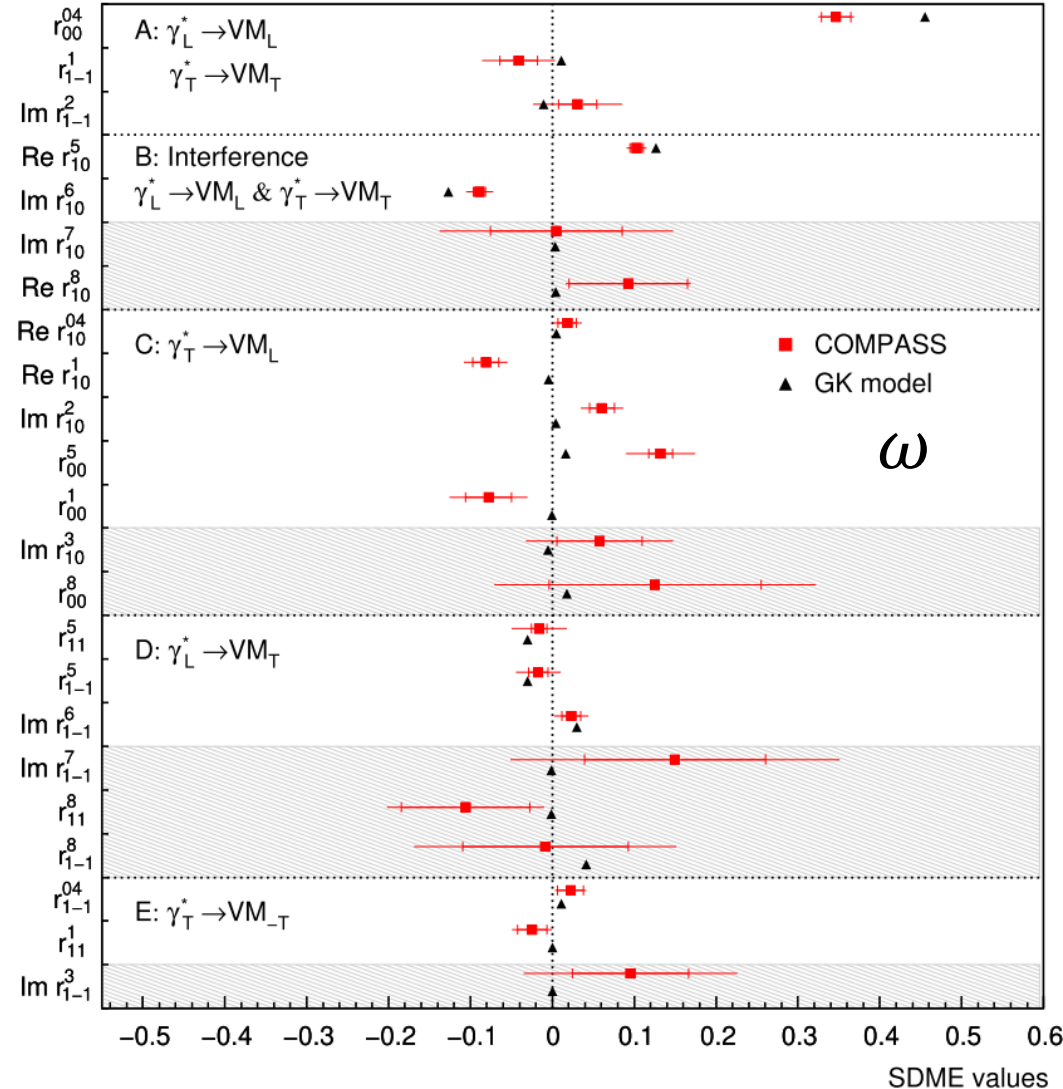
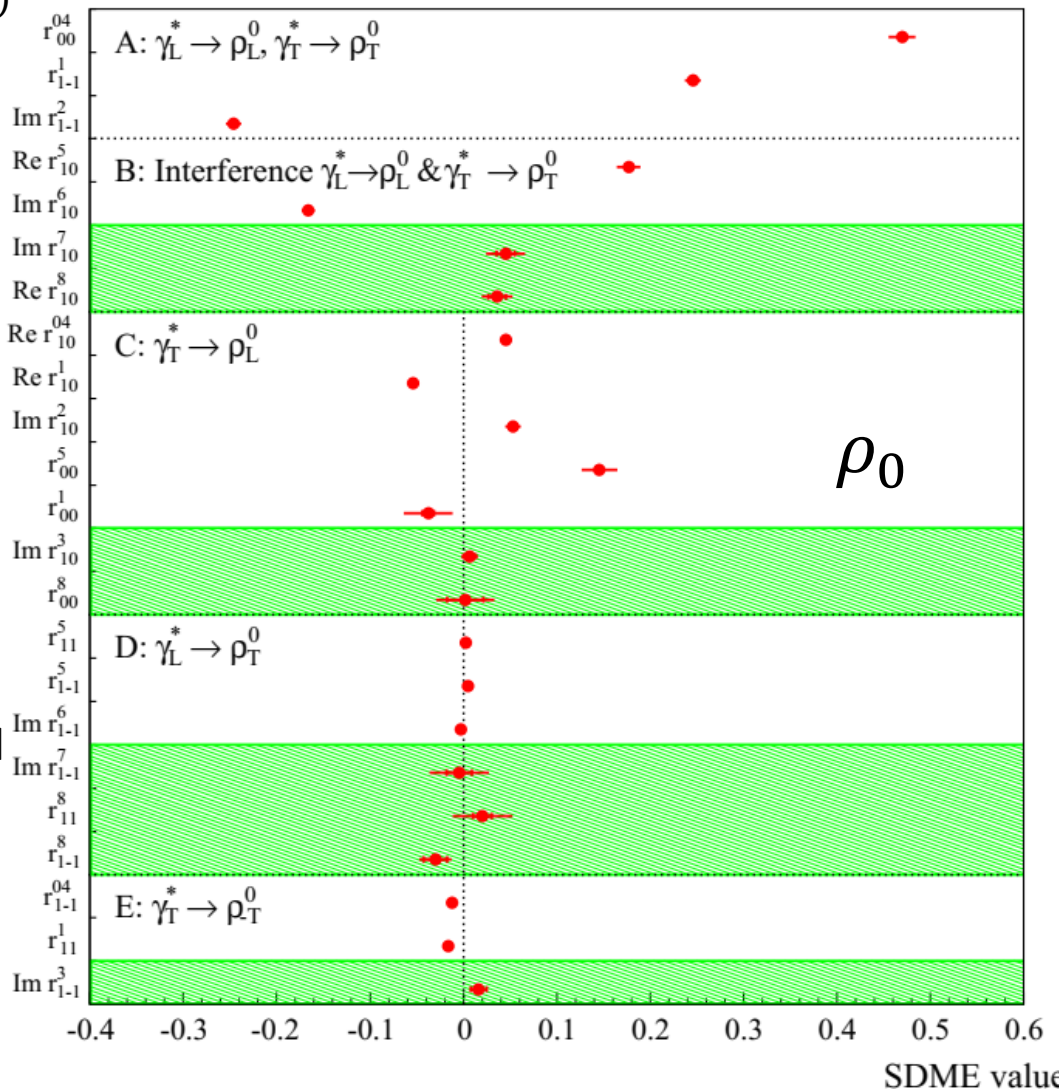
COMPASS preliminary

EPJC 81 (2021) 126

A, B, C, D, E classes corresponding to different helicity transitions

shaded areas show SDMEs related to beam polarization

GK model:
 Goloskokov and Kroll
 EPJA 50 (2014) 146
 parameters
 constrained mostly
 by HERMES results
 for ρ^0 and ω



Results: SCHC

❖ SCHC implies: $r_{1-1}^1 + \text{Im } r_{1-1}^2 = 0$ **OK**

$\text{Re } r_{10}^5 + \text{Im } r_{10}^6 = 0$ **OK**

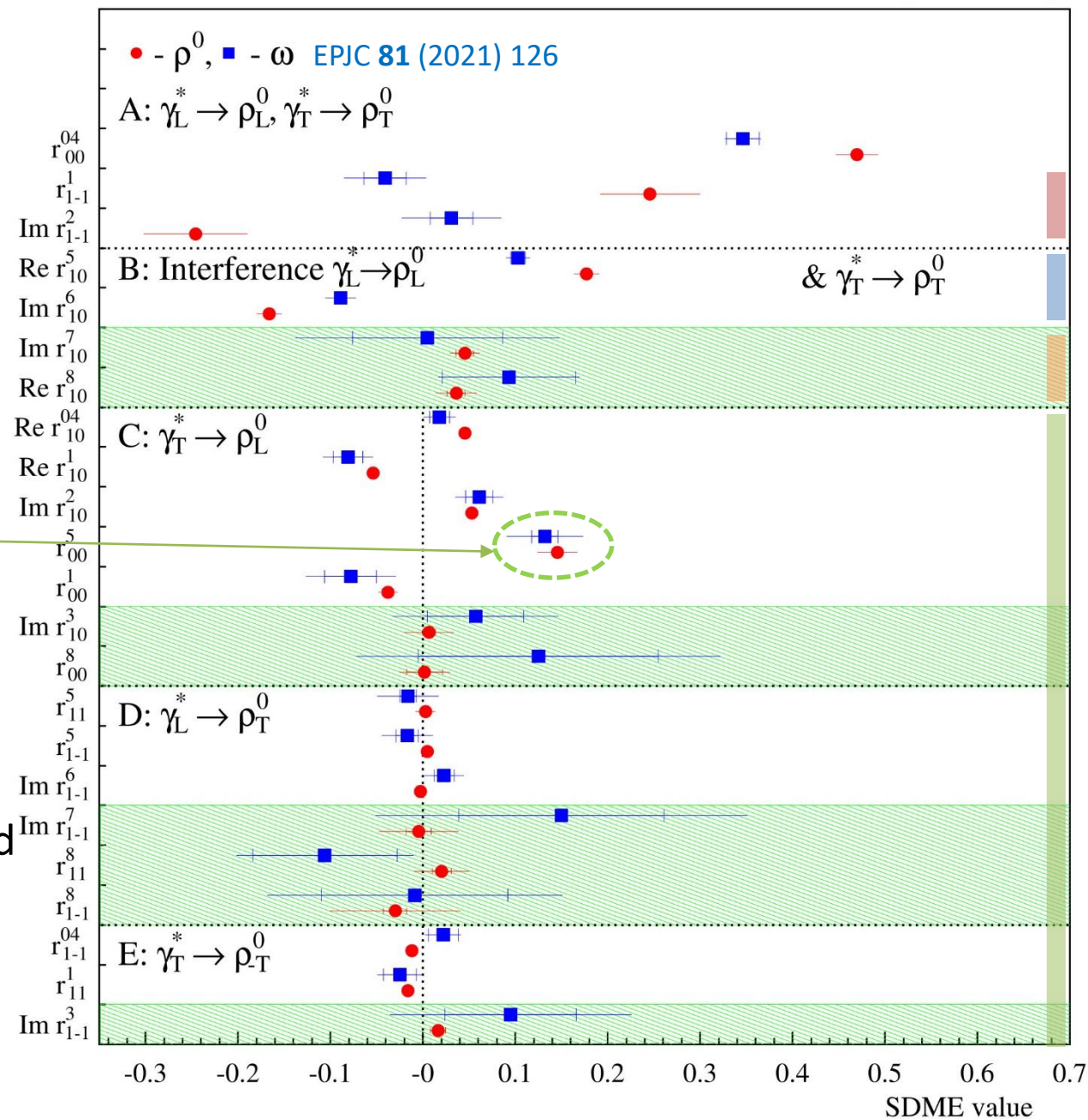
$\text{Im } r_{10}^7 + \text{Re } r_{10}^8 = 0$ **OK**

all elements of classes C, D, E should be 0

- ❖ SCHC violation in class C – transition $\gamma_T^* \rightarrow V_L$
- ❖ possible GPD interpretation **Goloskokov and Kroll, EPJC 74 (2014) 2725:**
- ❖ contribution of amplitudes depending on chiral-odd (“transversity”) GPDs $H_T, \bar{E}_T = 2\tilde{H}_T + E_T$

$$r_{00}^5 \sim \text{Re} \left[\langle \bar{E}_T \rangle_{LT}^* \langle H \rangle_{LL} + \frac{1}{2} \langle H_T \rangle_{LT}^* \langle E \rangle_{LL} \right]$$

- ❖ first term dominates, r_{00}^5 essentially probes \bar{E}_T



Results: Helicity-Flip NPE Amplitudes ρ^0

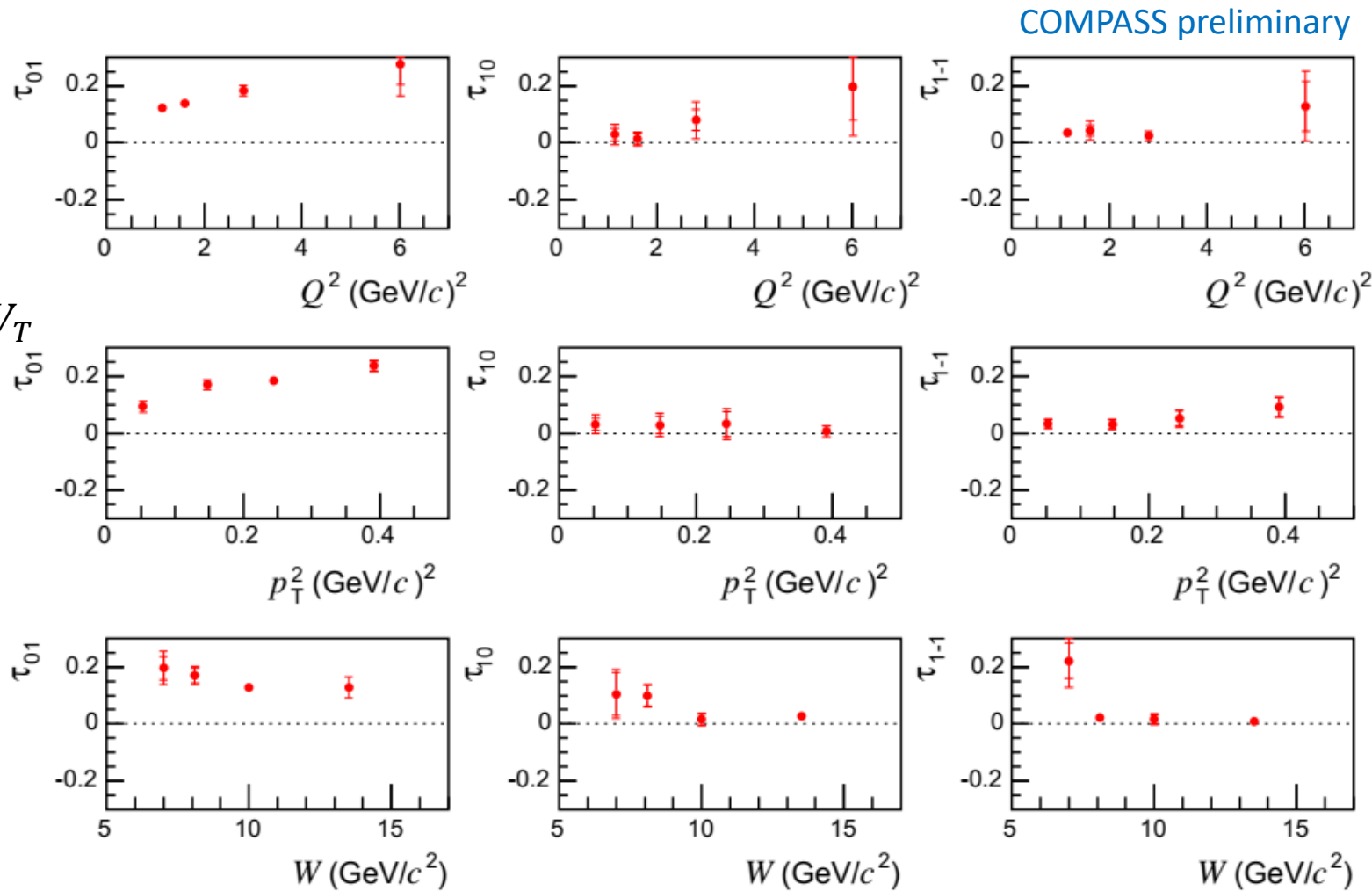
❖ described as $\tau_{ij} = \frac{|T_{ij}|}{\mathcal{N}}$

$$\tau_{01} \approx \sqrt{\epsilon} \frac{\sqrt{(r_{00}^5)^2 + (r_{00}^8)^2}}{\sqrt{2r_{00}^{04}}} \quad \gamma_T^* \rightarrow V_L$$

$$\tau_{10} = \frac{\sqrt{(r_{11}^5 + \text{Im}\{r_{1-1}^6\})^2 + (\text{Im}\{r_{1-1}^7\} - r_{11}^8)^2}}{\sqrt{2(r_{1-1}^1 - \text{Im}\{r_{1-1}^2\})}} \quad \gamma_L^* \rightarrow V_T$$

$$\tau_{1-1} = \frac{\sqrt{(r_{11}^1)^2 + (\text{Im}\{r_{1-1}^3\})^2}}{\sqrt{r_{1-1}^1 - \text{Im}\{r_{1-1}^2\}}} \quad \gamma_T^* \rightarrow V_{-T}$$

❖ only τ_{01} significantly differs from 0, consistent with SCHC violation in C, D, E



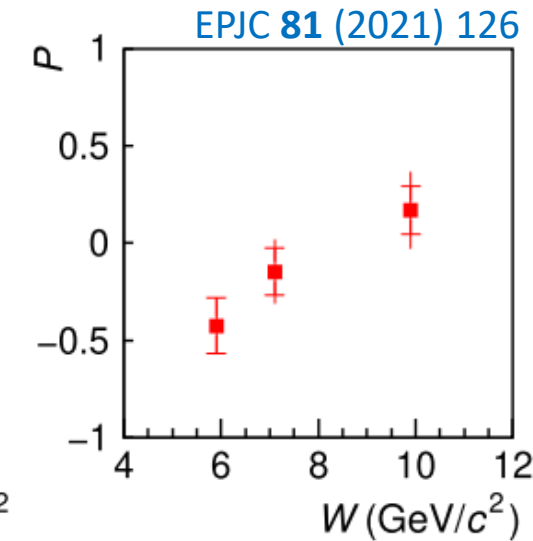
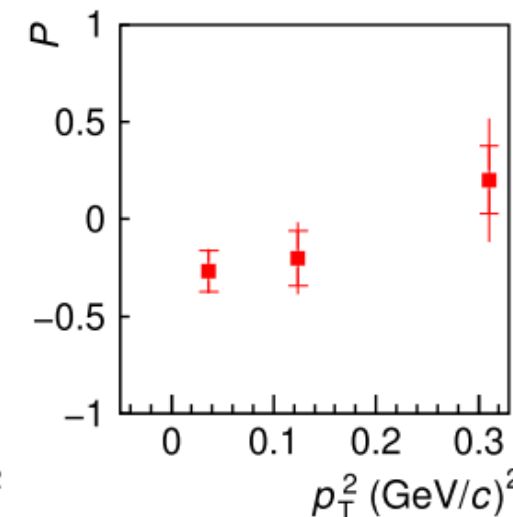
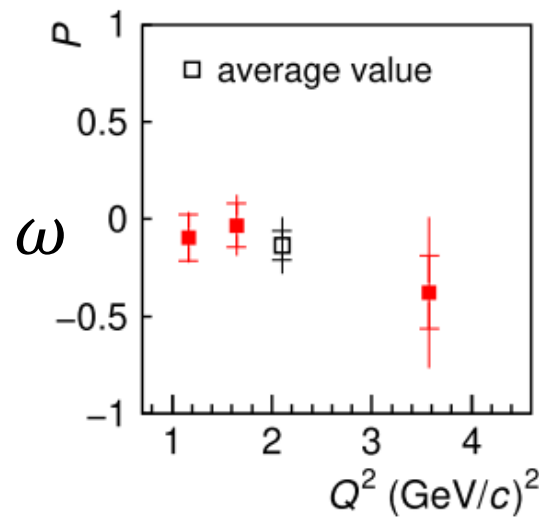
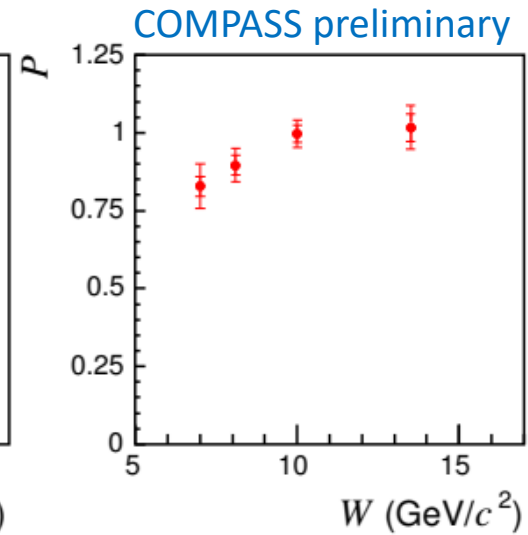
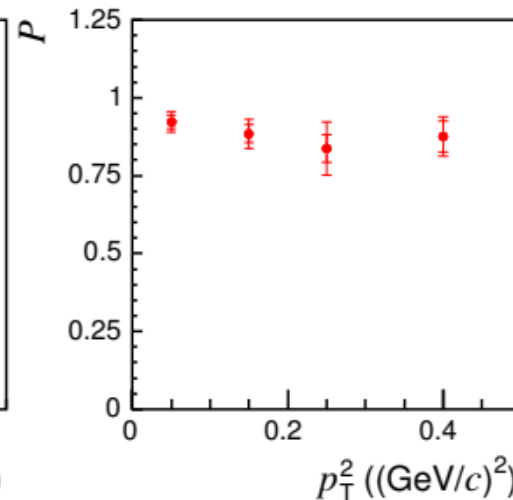
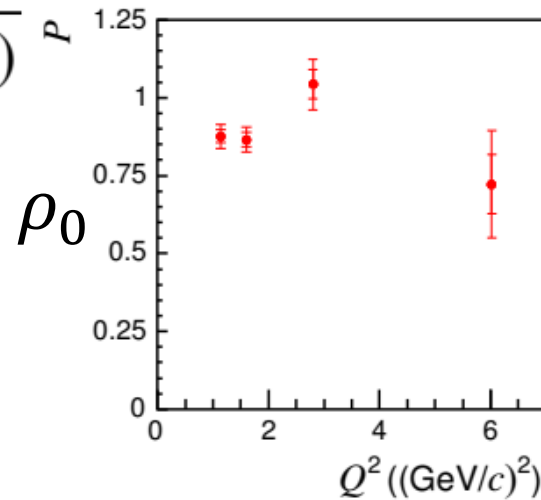
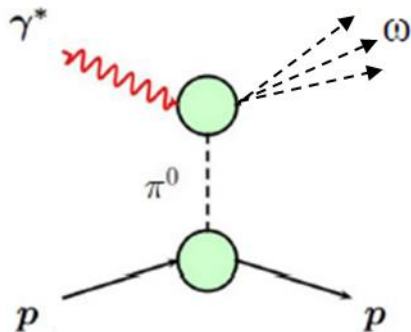
Results: NPE to UPE asymmetry

$$P = \frac{d\sigma_T^N(\gamma_T^* \rightarrow V_T) - d\sigma_T^U(\gamma_T^* \rightarrow V_T)}{d\sigma_T^N(\gamma_T^* \rightarrow V_T) + d\sigma_T^U(\gamma_T^* \rightarrow V_T)}$$

$$= \frac{2r_{1-1}^1}{1 - r_{00}^{04} - 2r_{1-1}^{04}}$$

❖ ρ_0 NPE dominance
NPE \rightarrow GPDs E, H

❖ ω NPE \approx UPE on average
UPE dominance at small W
and p_T^2
 \rightarrow GPDs \tilde{E}, \tilde{H}
+ pion pole
(dominant)



Results: Unnatural Parity Exchange contribution

$$u_1 = 1 - r_{00}^{04} + 2r_{1-1}^{04} - 2r_{11}^1 - 2r_{1-1}^1$$

$$u_1 = \sum \frac{4\epsilon|U_{10}|^2 + 2|U_{11} + U_{-11}|^2}{\mathcal{N}}$$

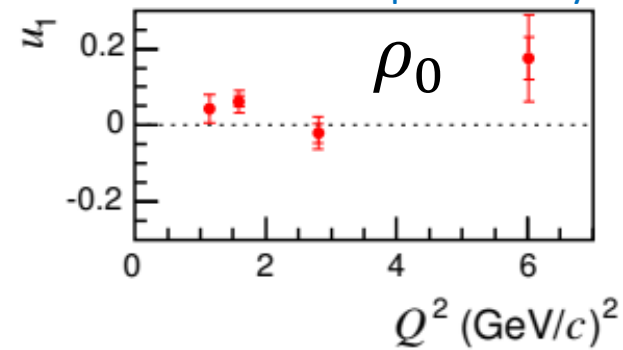
$$\tau_{UPE}^2 = (2\epsilon|U_{10}|^2 + |U_{01}|^2 + |U_{1-1}|^2 + |U_{11}|^2) / \mathcal{N} \approx u_1 / 2$$

- ❖ numerator in u_1 depends only on UPE amplitudes $\rightarrow u_1 > 0$
- ❖ ρ^0 very small UPE contribution observed
 - ❖ τ_{UPE}^2 0.03 averaged (UPE fractional contribution)
- ❖ ω large UPE contribution decreasing with increasing W in u_1
 - ❖ $\tau_{UPE}^2 = 0.5 \rightarrow 0.3$
- ❖ u_2 and u_3 consistent with zero

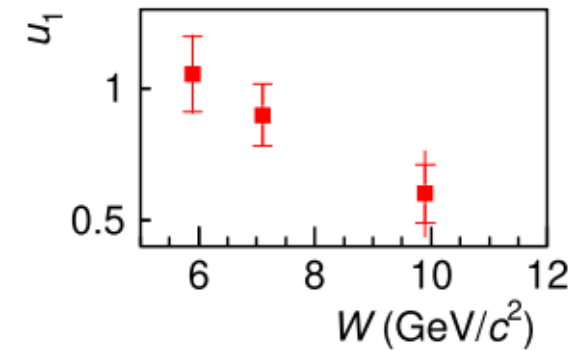
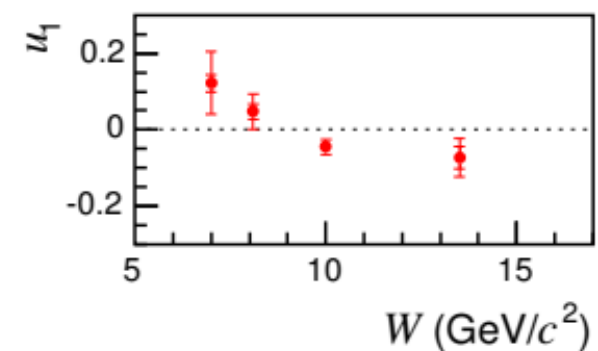
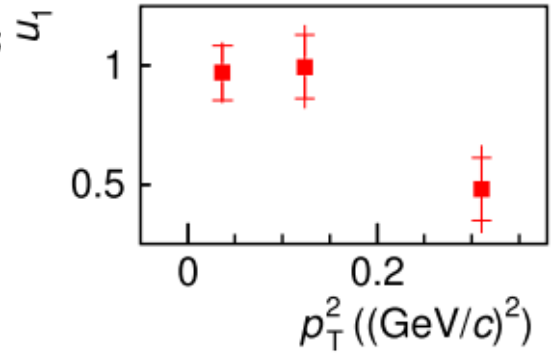
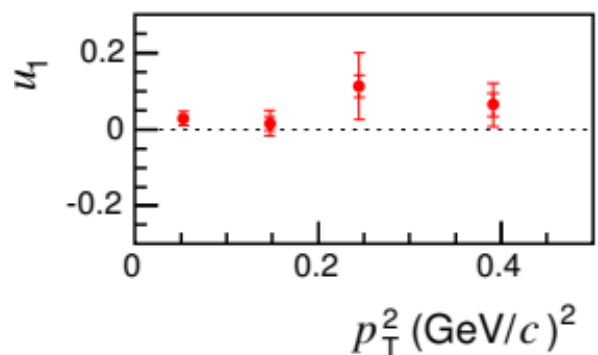
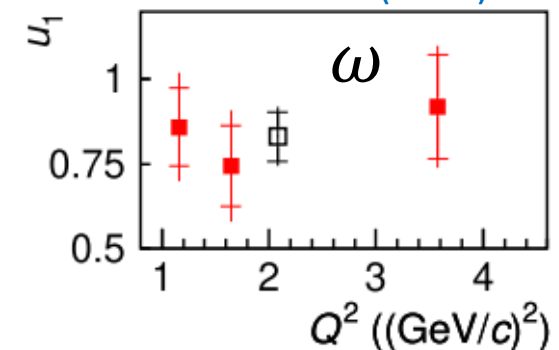
$$u_2 = r_{11}^5 + r_{1-1}^5$$

$$u_3 = r_{11}^8 + r_{1-1}^8$$

COMPASS preliminary



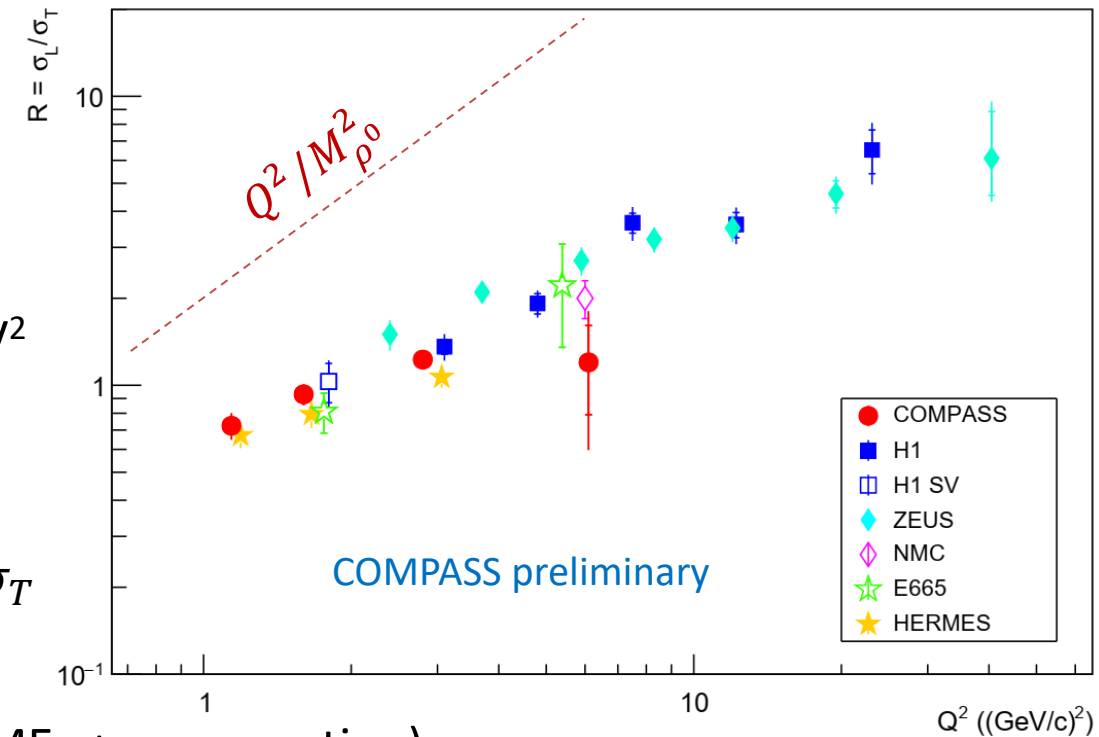
EPJC 81 (2021) 126



Summary and outlook

- ❖ results of exclusive π_0 cross-section show the importance of chiral-odd GPDs \bar{E}_T, H_T
- ❖ violation of SCHC hypothesis in transitions $\gamma_T^* \rightarrow V_L$ related to chiral-odd GPDs \bar{E}_T, H_T
- ❖ large UPE contribution in ω due to the pion pole (in contrast to ρ^0 where NPE dominates)
- ❖ ρ^0 longitudinal-to-transverse cross-section ratio

$$R = \frac{\sigma_L(\gamma_L^* \rightarrow V)}{\sigma_T(\gamma_T^* \rightarrow V)} \text{ in case of SCHC} = \frac{1}{\epsilon} \frac{r_{00}^{04}}{1 - r_{00}^{04}}$$
 - ❖ compared to the previous experiments with $Q^2 > 1.0 \text{ GeV}^2$
 - ❖ deviation from the pQCD LO prediction in $Q^2/M_{\rho^0}^2$:
due QCD evolution and q_T
 - ❖ transverse size effects of the meson smaller for σ_L than σ_T
- ❖ future:
 - ❖ 2016/17 data (on unpolarized LH₂ target): $\phi, \omega, J/\psi$ (SDMEs + cross-section)
 - ❖ 2022 data (on transversely polarized ^6LiD target): exclusive ρ^0 asymmetries for E^u and E^d separation



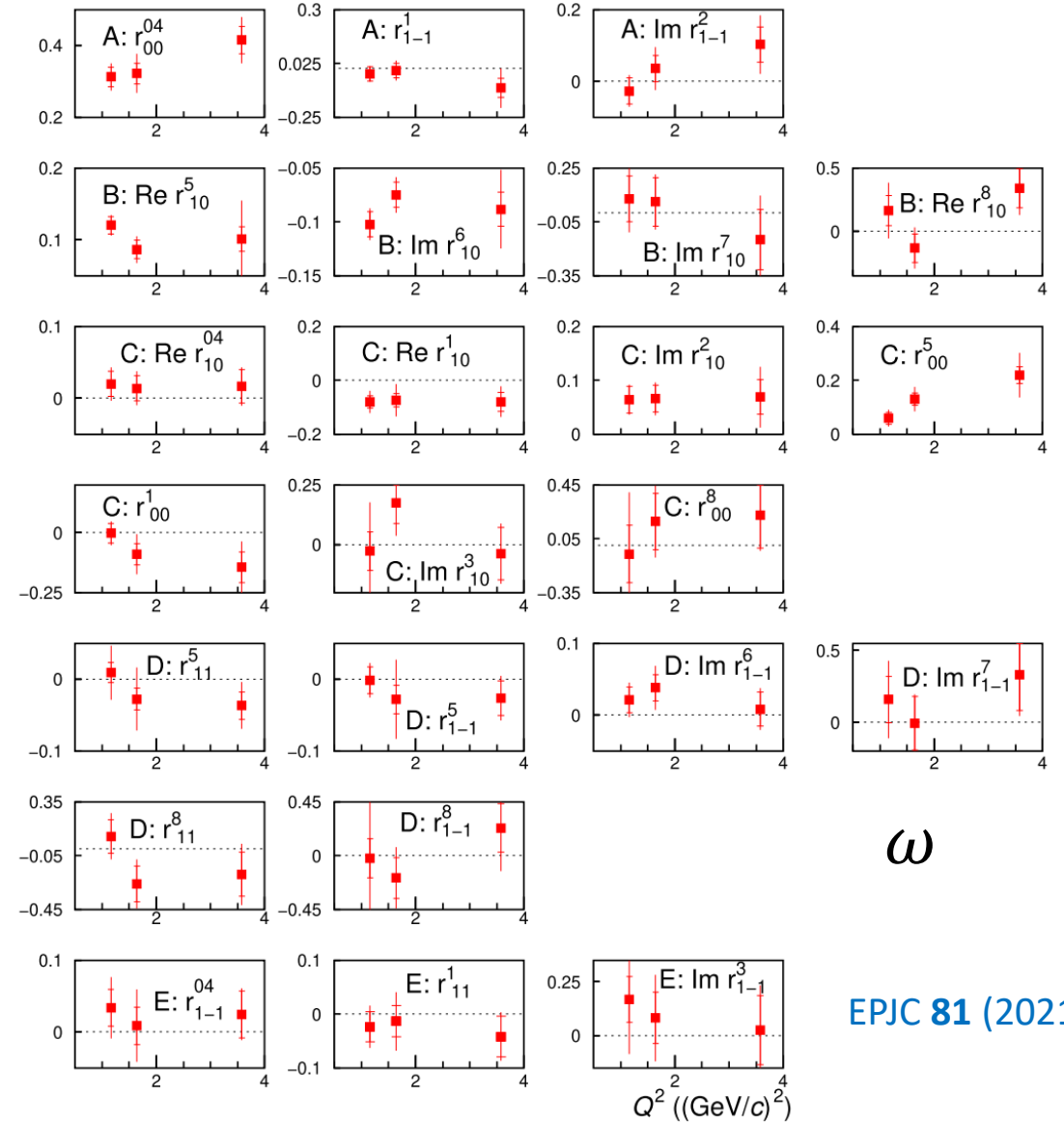
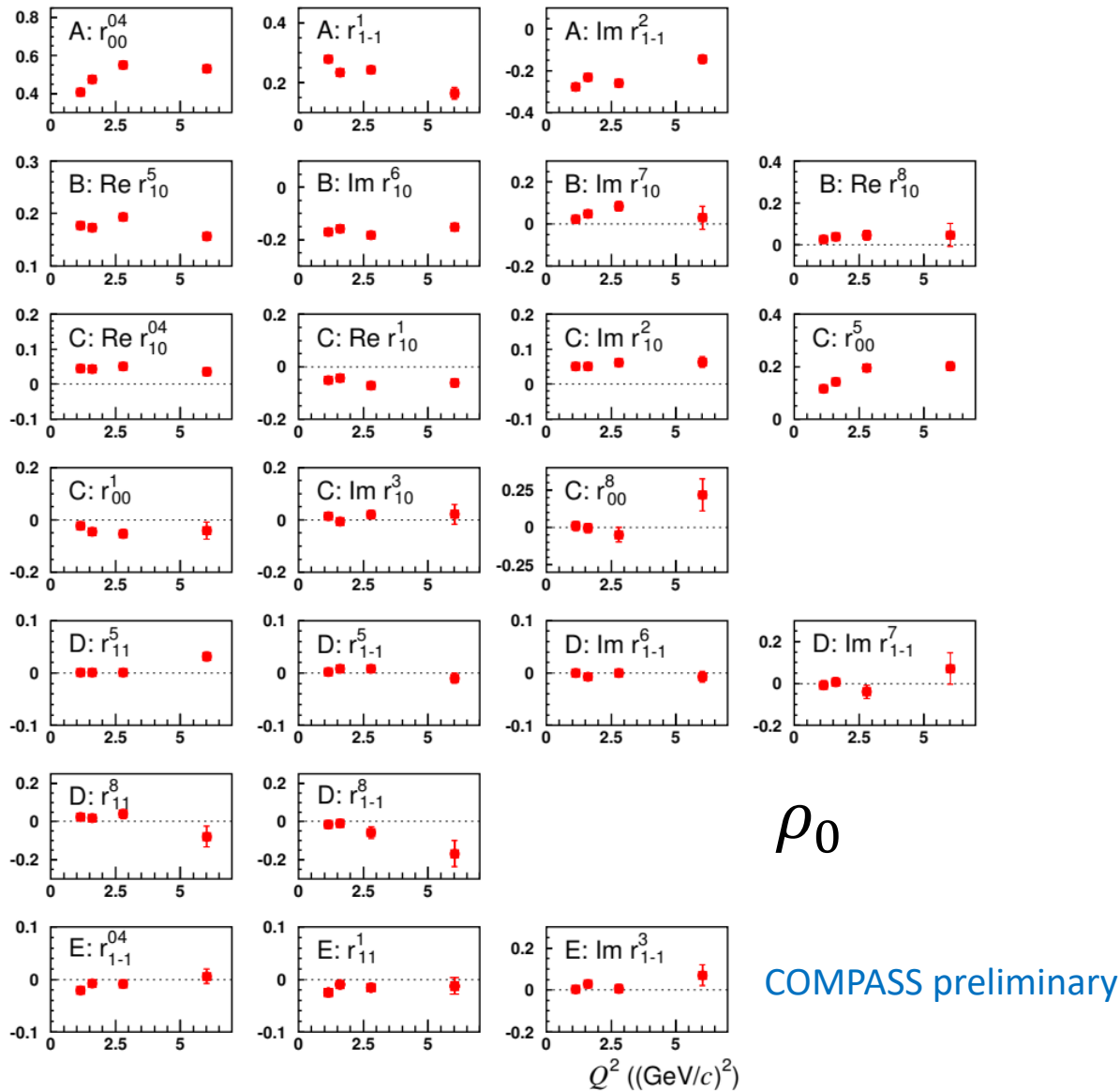
Thank you for your attention

GPD=?

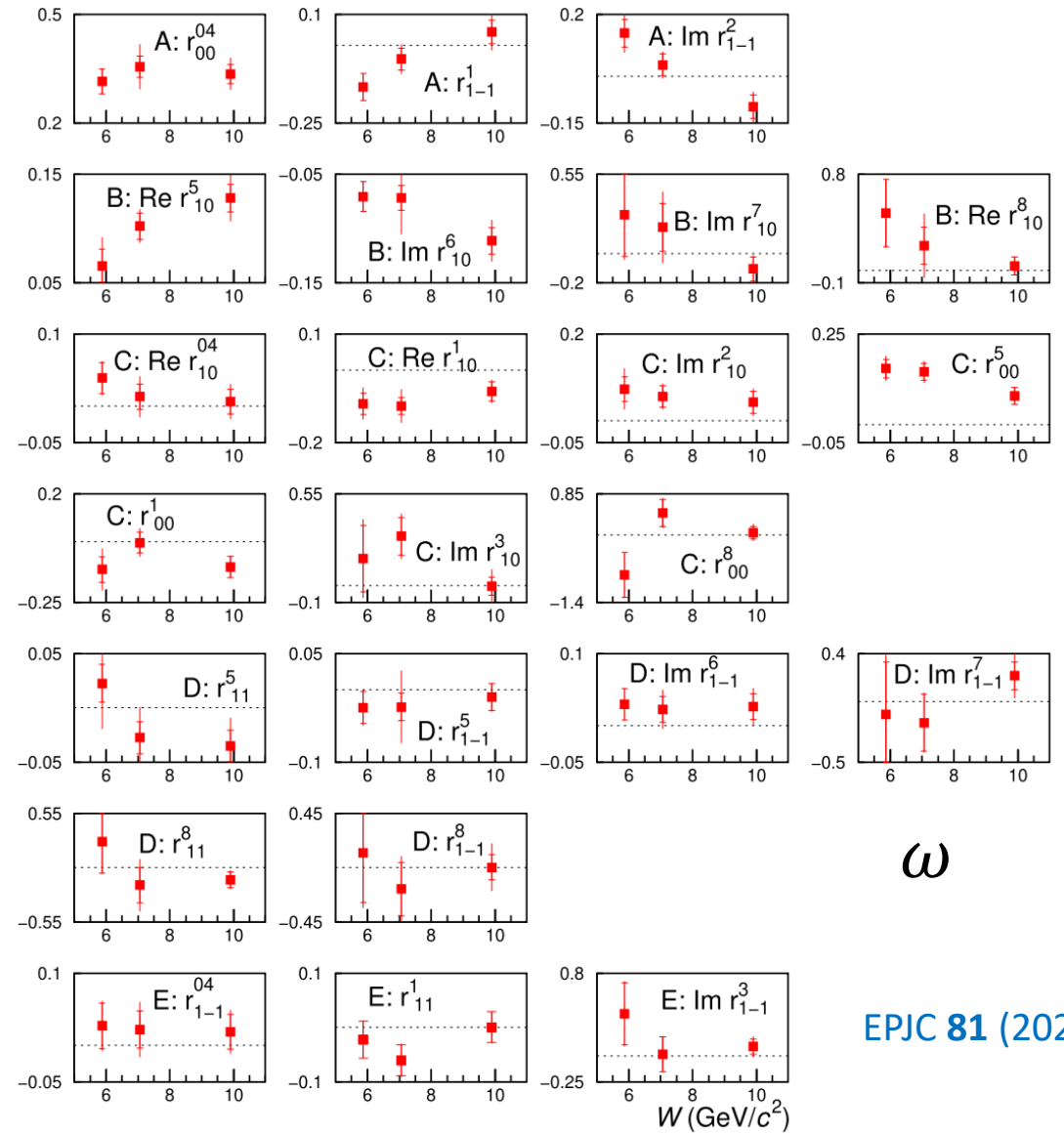
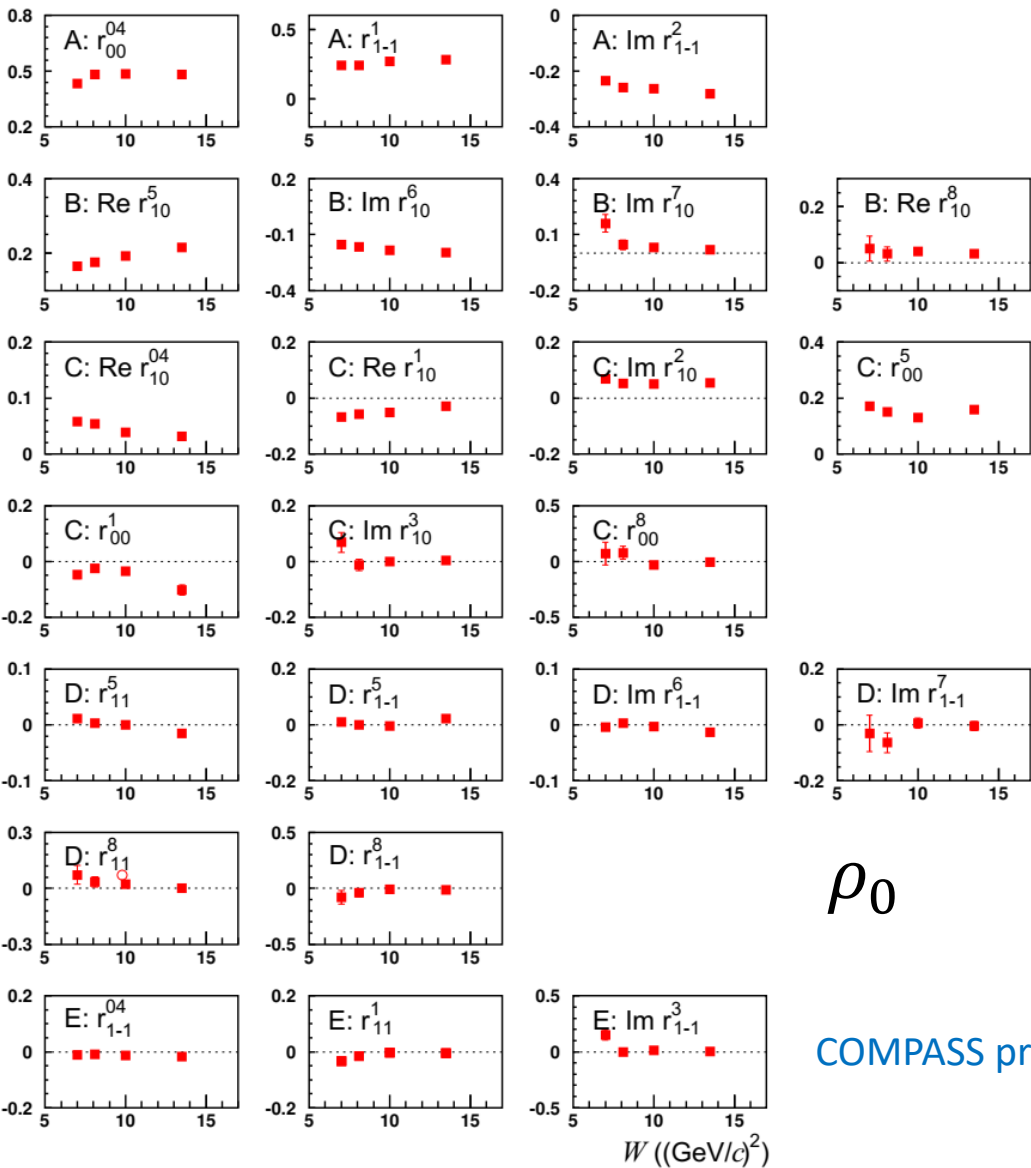
Abbreviation Finder

Acronym	Definition
GPD	Gallons Per Day
GPD	Guam Police Department
GPD	Glass Processing Days
GPD	SEE ALL >>

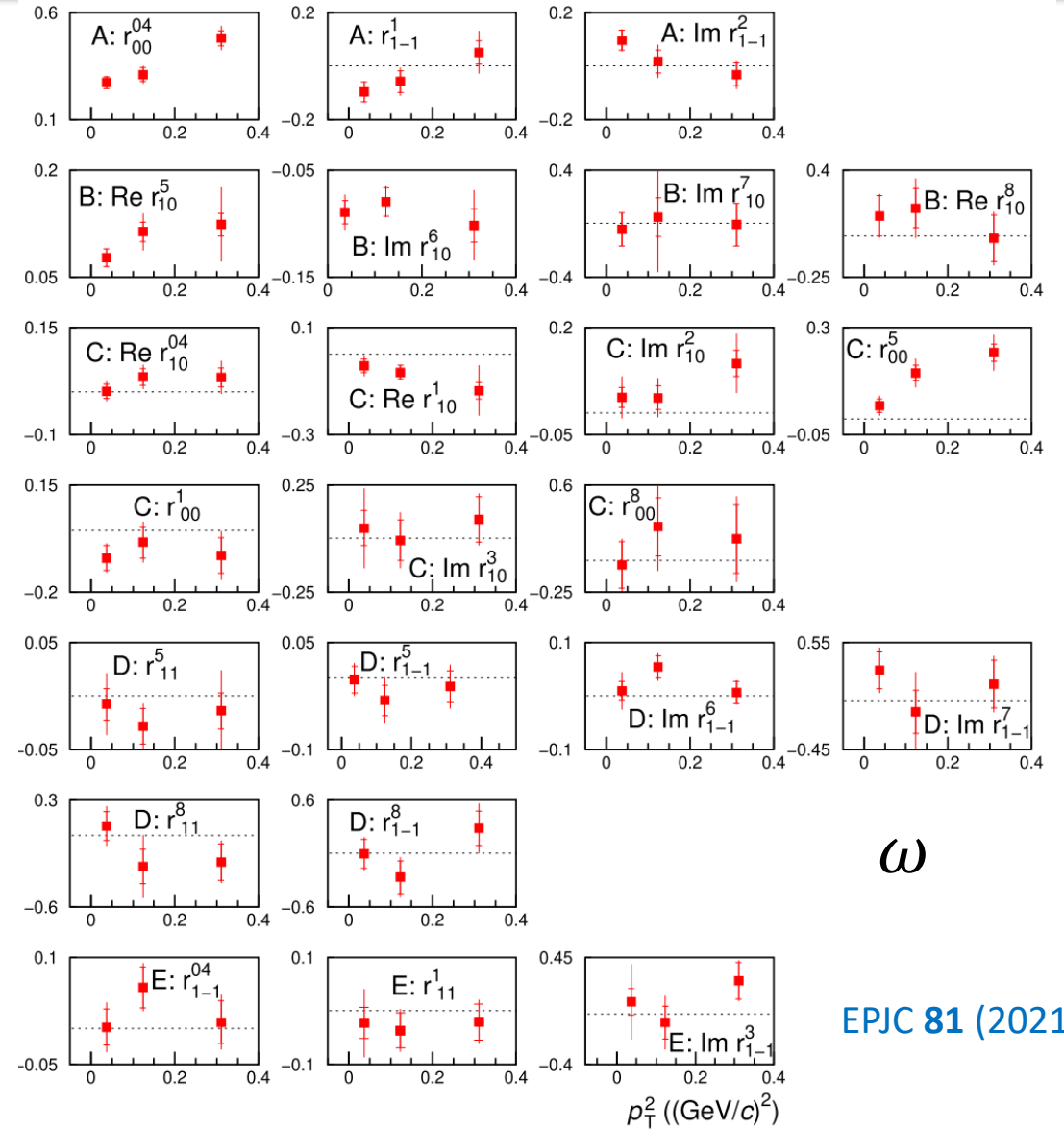
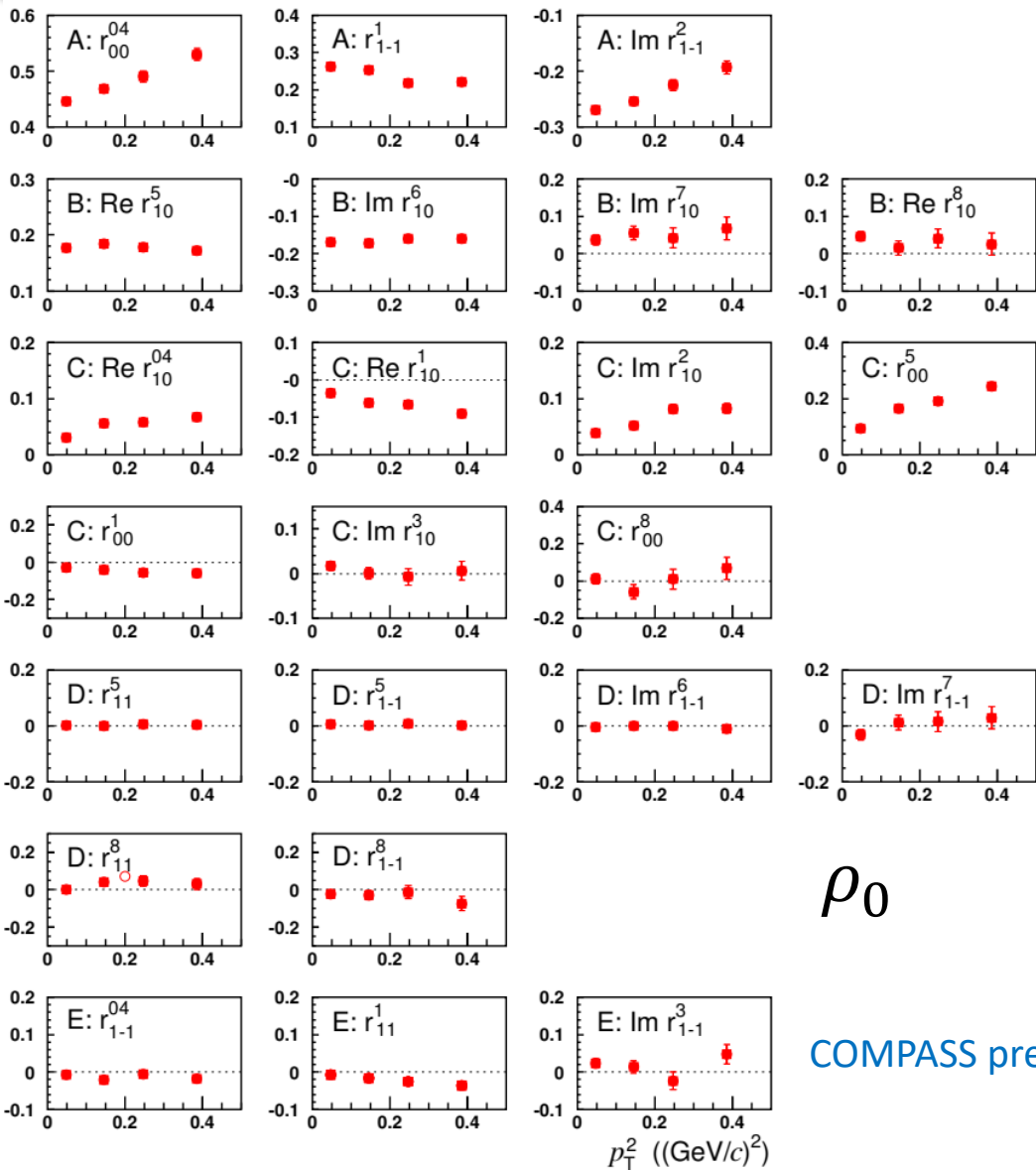
SDMEs dependences



SDMEs dependences



SDMEs dependences



SDMEs comparison with HERMES

HERMES SDMEs results:
 ω - EPJC **74** (2014) 3110,
 ρ^0 - EPJC **62** (2009) 659–695

